Crystal growth of air hydrates over 720 ka in Dome Fuji (Antarctica) ice cores: microscopic observations of morphological changes below 2000 m depth

Tsutomu UCHIDA,[1] Atsushi MIYAMOTO,[2] Atsushi SHIN'YAMA,[1] Takeo HONDOH[2]

[1]*Division of Applied Physics, Faculty of Engineering, Hokkaido University, Sapporo 060-8628, Japan*
E-mail: t-uchida@eng.hokudai.ac.jp
[2]*Institute of Low Temperature Science, Hokkaido University, Sapporo 060-0819, Japan*

ABSTRACT. Air-hydrate crystals store most of the ancient air contained in deep ice sheets. We carried out microscopic observations of air-hydrate crystals below 2000 m depth within the ice core from Dome Fuji, Antarctica, to obtain their number and size distributions. We found that the number density continuously decreased with depth, whereas the average size increased, in contrast to findings from shallower depths. In addition, the characteristic perturbations in both number density and average size distribution with climatic changes almost disappeared, although they are clearly observed in shallow cores. These results indicate that the air-hydrate crystals grow considerably in deeper parts of the ice sheet, and this growth is accompanied by the diffusion of air molecules in the ice. The permeation coefficient of the air molecules in the ice sheet was estimated from the geometric parameters of the air-hydrate distributions. This is the first practical evidence comparable to the previous model estimations. It allows us to evaluate the impacts of the air-molecule migration in the ice sheet on the paleoclimatic information recorded in the deep ice cores.

1. INTRODUCTION

Ancient atmospheric gases are trapped in the form of air bubbles in polar ice sheets when the accumulated snow transforms into ice without melting. Paleoclimatic and environmental records spanning several hundred kiloyears (ka) have been acquired from continuous long ice cores retrieved from the Antarctic ice sheet (Johnsen and others, 1972; Petit and others, 1999; Watanabe and others, 2003; EPICA Community Members, 2004, 2006). Two continuous long ice cores have been drilled at the summit of Dome Fuji station, Antarctica. The first was drilled from the surface to 2503 m depth between 1993 and 1997 (Dome-F Deep Coring Group, 1998); the second was drilled to 3035 m between 2005 and 2007 (Motoyama, 2007). The deepest ice core has been analyzed to ~720 ka BP (Motoyama and others, 2007; Goto-Azuma and others, 2008). Data from analysis of these ice cores are expected to contribute substantially to the paleoclimatic and environmental records.

Air bubbles and air hydrates in the polar ice cores are attracting considerable interest because they provide the most direct record of past atmospheric gas compositions. Air bubbles in ice sheets are compressed with depth and gradually transform into clathrate hydrates below a certain depth at which the hydrostatic pressure becomes greater than the dissociation pressure of the clathrate hydrate at the in situ temperature (Miller, 1969; Shoji and Langway, 1982). Air hydrate is a stable solid clathrate compound (Van der Waals and Platteeuw, 1959; Sloan and Koh, 2008) with a Stackelberg's structure II (Hondoh and others, 1990). Although air-hydrate crystals are small and transparent, they contain a volume of air molecules 150 times larger than an equivalent volume of air. This is $>10^6$ times larger than the equilibrium concentration of air molecules in the ice matrix. Therefore, most of the ancient air molecules are considered to be stored in air-hydrate crystals in the deep ice sheets.

Systematic observations of natural air hydrates were carried out on ice cores retrieved from deep boreholes at Vostok station, East Antarctica (Lipenkov and Salamatin, 1989; Lipenkov and others, 1989; Uchida and others, 1994a,b; Lipenkov, 2000). They revealed that the air inclusions changed phase from bubbles to clathrate hydrates below ~550 m depth, which corresponded to the thermodynamic equilibrium state of air hydrate (Miller, 1969), and that the geometric configuration of the air-hydrate distributions (e.g. shape, number concentration, average size) varied with depth. The phase transition occurred gradually over several hundred meters below 550 m, which we call the transition zone, where air bubbles and air-hydrate crystals coexist. The depth distribution of the geometric parameters of the air-hydrate crystals also indicated that their number and size profiles fluctuate in parallel with climatic changes and are mainly a result of the original characteristics of the air-bubble distribution (Lipenkov, 2000) and the heterogeneous nucleation of air-hydrate crystals on air bubbles induced by the micro-inclusions (Ohno and others, 2010). Therefore, air-hydrate crystals contain not only ancient air molecules in their structures, but also records of climatic change in their distribution parameters.

The distribution of air inclusions at depths between 182 and 2101 m in the Dome Fuji ice core was observed by Ohno and others (2004). They found that the transition zone lies between 500 and 1250 m depth. It was confirmed that below the transition zone no air bubbles exist and the number and size distributions of the air-hydrate crystals provide climate information. Raman spectroscopic measurements of air inclusions (Ikeda and others, 1999; Ikeda-Fukazawa and others, 2001) revealed that the composition of the air (N_2/O_2 ratio) in the inclusions changes significantly with depth in the transition zone. This composition change is restored to its original ratio at the bottom of the transition zone, which suggests that the change is caused by the

https://doi.org/10.3189/002214311798843296 Published online by Cambridge University Press

fractionation during the air bubble–hydrate transformation (Lüthi and others, 2010).

The depth distribution of the geometric parameters and the gas composition of the air-hydrate crystals suggest that the air molecules trapped in the air inclusions migrate in the ice. The major driving force behind this air migration is the phase transition between bubbles and air hydrates, and the subsequent crystal growth of the air hydrates is supplemented by air molecules from the surrounding air bubbles (Uchida and others, 1994c). Even below the transition zone, air-hydrate crystals are found to grow slightly (Uchida and others, 1994a; Lipenkov, 2000). The crystal growth of air hydrates is thought to be controlled by air-molecule diffusion through the ice crystal (Salamatin and others, 1998). If significant air-molecule diffusion occurs, it will create a serious problem for ice-core analysis because the air-hydrate crystal will no longer act as a reliable container of ancient air. Therefore, the estimation of the air-molecule diffusion through ice in parallel with the air-hydrate crystal growth is important for studies on ancient climatic change using deep ice cores. However, precise estimation is difficult because the air molecule diffusion is too small to be examined in the timescale of a laboratory study. In addition, since the model predictions are based on a purified system such as a single crystal (Ikeda and others, 2000a; Ikeda-Fukazawa and others, 2004a,b), it is difficult to directly apply these predictions to natural conditions that contain grain boundaries, impurities, lattice defects, etc. The analysis of air-hydrate distribution, especially in the deep part of the Dome Fuji ice core, is very useful for investigating such slow processes because the ice sheet at the dome location preserves the ice and inclusions over a very long time. Thus, it is considered to be a natural laboratory for observing long and quasi-equilibrium reactions.

In the present study, the distributions of air-hydrate crystals from the Dome Fuji deep ice core are measured at depths between 2048 and 3024 m and combined with previous data obtained from shallow depths (Ohno and others, 2004), to complete the depth profiles of air-hydrate crystal evolution over ~720 ka. Our study also provides insight into the effect of air-molecule migration on ice-core analyses.

2. METHODS

Sample preparation and optical microscopic observations were carried out in a cold room at ~258 K. Forty-nine thin sections of ice 5 mm thick, 45 mm wide and 100 mm long were prepared from locations along the axis of the ice core. Six ice pieces were selected from the first Dome Fuji ice core (Dome-F Deep Coring Group, 1998) at depth y between 2048 and 2430 m; 43 ice pieces were selected from the second core (Motoyama and others, 2007) between 2404 and 3024 m. These ice cores were carefully transported from the drilling site where the average temperature was ~243 K (Dome-F Deep Coring Group, 1998) to a cold storage room at the Institute of Low Temperature Science, Hokkaido University, Japan, where the storage temperature was lower, ~223 K, in order to inhibit post-drilling air-hydrate decomposition (Uchida and others, 1994d). The high quality of ice, and the successful control of the temperature during the transportation were verified by volume expansion measurements (Miyamoto and others, 2009). Six shallower ice pieces were analyzed to compare the results of our observations with previous results (Ohno and others, 2004) and to fill the gap in the data at depths between 2000 and 2500 m.

The experimental procedures and calculation methods employed for the geometrical parameters of distribution are essentially the same as those used in previous works (Uchida and others, 1994a; Lipenkov, 2000; Ohno and others, 2004) and are explained here briefly. The shape and size of the air-hydrate crystals included in the observation area of 1.4 mm width, 5 mm thickness and 100 mm length (~700 mm^3; referred to as the optical line) within a thin section cut parallel to the depth direction were measured using an optical microscope (Olympus, model BH2-UMA) with a magnification range ×100 to ×400. One to three optical lines were measured on each thin section to obtain a sufficient number of air hydrates (>200). We determine their number concentrations, N, mean size (average radius, r) and shape classifications. The types of air-hydrate crystals were classified into five groups (Fig. 1a–e). The size of an air-hydrate crystal is expressed by the radius of the sphere of the equivalent cross section obtained by using either a spherical or an ellipsoidal approximation. The average size of the air-hydrate crystals included in a thin section was estimated by fitting a log-normal function, $f_{LN}(r)$, to each size distribution obtained in the section (OriginLab Co., OriginPro 8.5.0J). We also checked both the spatial heterogeneity of the air-hydrate distribution in each thin section and the reproducibility of our measurements by comparing the measurement obtained from three optical lines for a thin section. Details of the estimation of measurement uncertainties are given in Appendix A. Because the average size of air-hydrate crystals included in the ice pieces from shallower depths was calculated by a different method (Ohno and others, 2004), we recalculated the average radius of the air-hydrate crystals by fitting a log-normal function, $f_{LN}(r)$.

3. RESULTS AND DISCUSSIONS

3.1. Depth variations of number concentration, *N*, and mean radius, *r*, in Dome Fuji ice core

Most (>90%) of the air-hydrate crystals were spherical (Fig. 1a) or ellipsoidal (Fig. 1b), even in the deep part of the ice core. This tendency is similar to that observed in previous studies of other deep ice cores in Antarctica (Uchida and others, 1994a; Lipenkov, 2000; Ohno and others 2004). There were few (<10%) faceted crystals (Fig. 1d), a common shape in the transition zone (Ohno and others, 2004) and an indicator of active crystal growth (Hondoh, 1989; Lipenkov, 2000). These results suggest that crystal growth in the region below the transition zone is not as active as in the transition zone.

The variation of N and r with depth in the Dome Fuji ice core is shown with solid circles in Figure 2a and b, respectively, along with results from previous work (Ohno and others, 2004). The figure shows that at depths of ~2000 m, where we consider the measurement uncertainties are 8.6%, the values obtained in the present study agree with those obtained in a previous work (Ohno and others, 2004; see Appendix A). The size distributions of both measurements are similar (see Fig. 10 in Appendix A). Therefore, we believe that a complete profile of the air-hydrate distribution can be obtained for the entire depth of the Dome Fuji ice core.

https://doi.org/10.3189/002214311798843296 Published online by Cambridge University Press

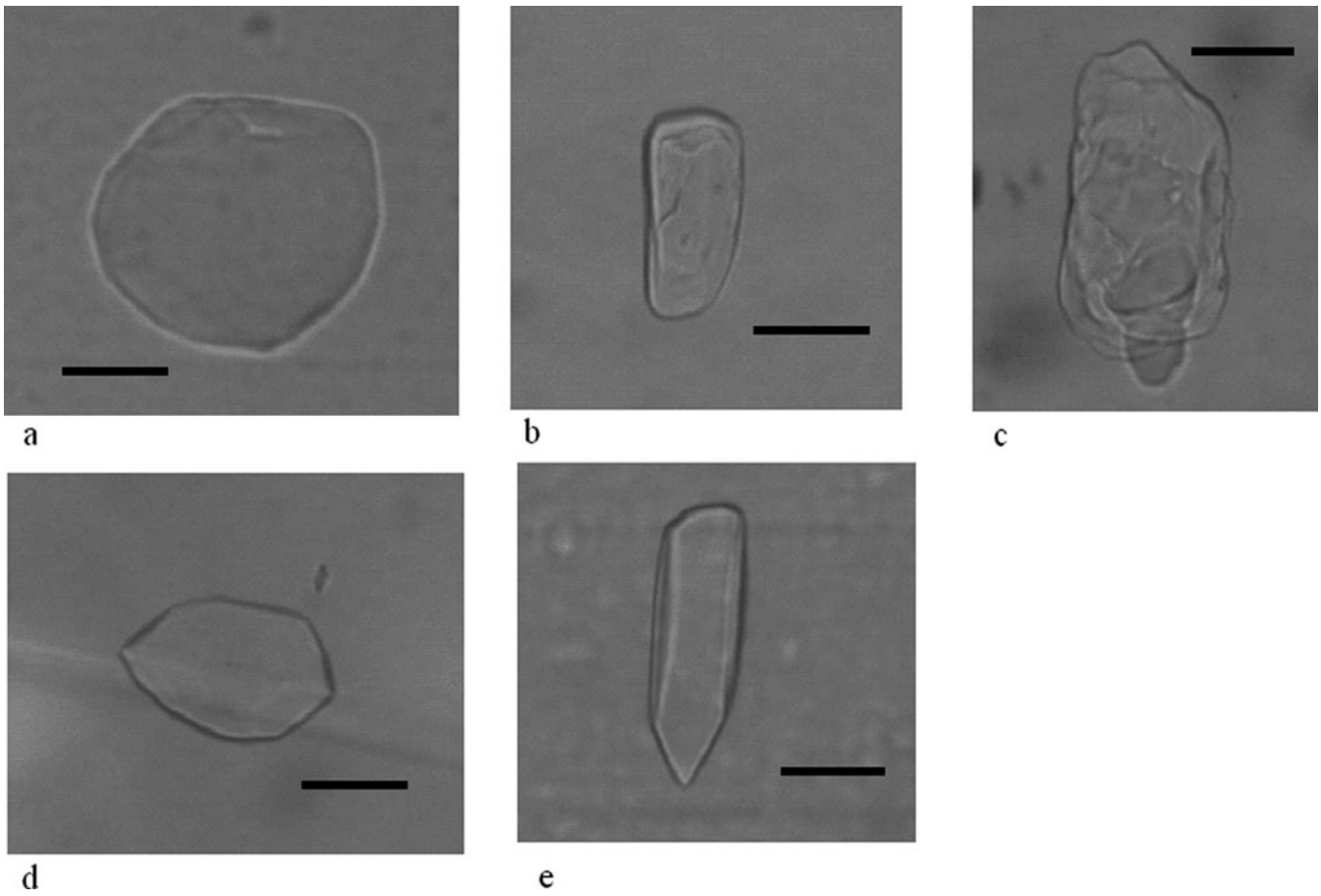

Fig. 1. Typical air-hydrate crystal shape (with 100 μm scale bar): (a) spherical, (b) ellipsoidal, (c) irregular, (d) faceted (the center line is the ice grain boundary) and (e) rod-like.

A comparison with the data obtained at shallow depths (>2000 m) reveals that *N* decreases continuously with depth. The sensitivity of the *N* distribution with climatic change appears to diminish in the deeper region. This obvious decrease in *N* at greater depths has not been reported in other deep ice cores (e.g. below 2000 m in Vostok ice (Lipenkov, 2000)). The depth distribution of the average radius *r* also indicates a distinct profile, similar to that observed in the *N* profile. The depth distribution of *r* increases clearly and continuously with depth. The variation of *r* with climatic change also weakens, as observed in the *N* profile. Although a slight increase in *r* has been reported previously in the deep ice cores in Antarctica (Uchida and others, 1994a,b; Lipenkov, 2000; Ohno and others, 2004) and in Greenland (Pauer and others, 1999), it is difficult to say whether or not these slight increases in *r* were caused by climatic fluctuations. Thus, we believe that the increase in *r* in the deeper regions evident in the present study has not been previously reported.

Comparing the depth profiles of *N* and *r* below the transition zone, we observe that with depth the air-hydrate crystals in the Dome Fuji ice core decrease in number and increase in size, especially deeper than ~2500 m. In addition to the change in the depth profile, the climatic information in both the *N* and *r* distributions gradually diminishes with depth. $\delta^{18}O$ measurements and chronological studies on the Dome Fuji ice core (Kawamura and others, 2007) indicate that large glacial terminations exist at ~1800 m (termination II) and 2500 m (termination IV), respectively. Figure 2a and b show a relatively large *N* peak and small *r* drop at these depths. However, the intensity of the perturbations from the general trend is smaller in termination IV than in II. The crystal size distributions support these results (Figs 13 and 14 in Appendix B). This is also supported by the correlation diagrams between $\delta^{18}O$ (Kawamura and others, 2007; Motoyama and others, 2007) and *N* (Fig. 3a) and *r* (Fig. 3b). This figure indicates strong relationships between $\delta^{18}O$ and the air-hydrate parameters *N* and *r* at depths of 1200–2500 m, as predicted in previous studies (Uchida and others, 1994a; Pauer and others, 1999; Lipenkov, 2000; Ohno and others, 2004). These correlations are the result of the number and size variations of the air bubbles originating at shallower depths, as well as the climatic changes (Uchida and others, 1994; Lipenkov, 2000). However, both the *N* and *r* values in the deeper parts clearly deviate from the linear relationship. The climatically induced fluctuations are predicted to be reduced by the preferential growth of larger crystals in the deep ice sheet (Uchida and others, 1994; Salamatin and others, 2003). Therefore, it is considered that the unique distributions of *N* and *r* below 2500 m are not related to climatic change but are caused by modulation of the air-hydrate crystals during long-term storage in the ice matrix.

A comparison of the depth distribution data of the air-hydrate crystals at 3310 m obtained from the Vostok ice core (Uchida and others, 1994a; Lipenkov, 2000) clearly shows the disappearance of the strong relationship between the geometrical parameters of the air-hydrate crystals and $\delta^{18}O$. This observation suggests that the disappearance of

https://doi.org/10.3189/002214311798843296 Published online by Cambridge University Press

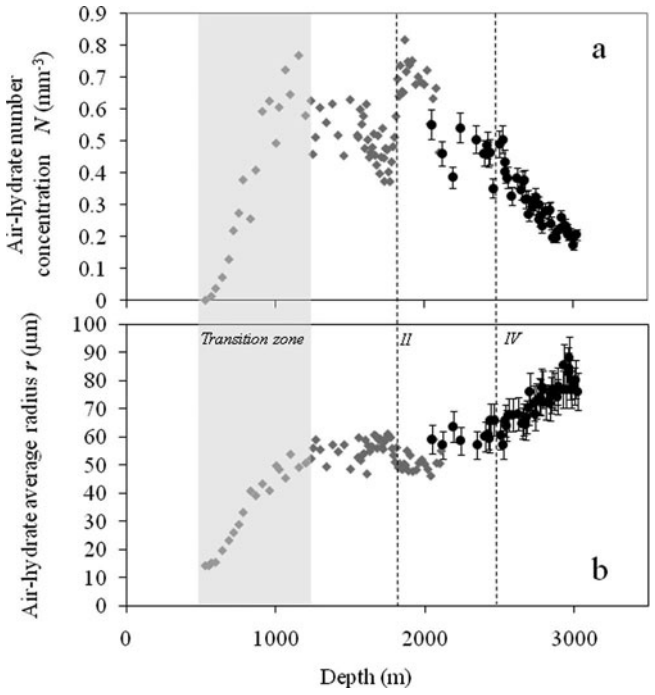

Fig. 2. Depth profiles of (a) air-hydrate number concentration N (solid circles: obtained in the present study; solid diamonds: obtained by Ohno and others, 2004) and (b) air-hydrate average radius r (solid circles: obtained in the present study; solid diamonds: obtained by Ohno and others, 2004). The hatched area indicates the transition zone. The dashed lines are the glacial terminations II and IV. The experimental uncertainties are shown by the error bar on one of the data points of the present study in each figure (estimation of the uncertainties is discussed in Appendix A).

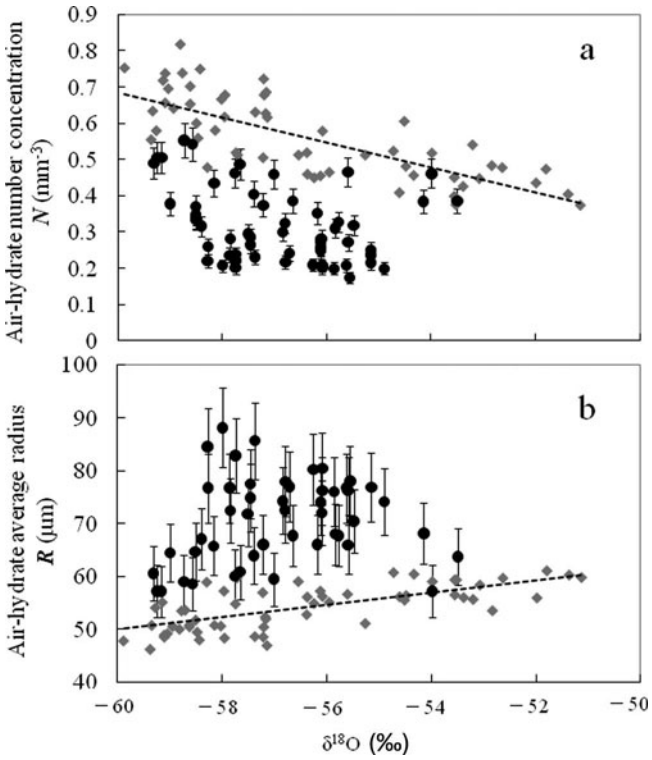

Fig. 3. Relations between $\delta^{18}O$ (Kawamura and others, 2007; Motoyama and others, 2007) and (a) number concentration N and (b) average radius r (solid circles: obtained in the present study; solid diamonds: obtained by Ohno and others, 2004). The dashed line in each panel is the linear regression between $\delta^{18}O$ and N or r at depths of 1200–2500 m, which suggests a strong relation between them at that depth range.

climate-related perturbation in the geometrical properties is caused not only by the depth and ice temperature but also by the age of the ice. The disappearance of the climate-related variations in the air-hydrate distributions in the Dome Fuji ice core becomes obvious at depths below 2500 m, or for ages greater than 400 ka BP (Kawamura and others, 2007).

3.2. Changes in the distribution of air-hydrate crystals in the deep ice sheet and their impacts on ancient climate information in an ice core

The depth profiles of the geometrical properties of air-hydrate crystals are developed mainly as a result of the crystal growth of air hydrates in the deep ice sheet (Uchida and others, 1993, 1994a,b; Lipenkov, 2000; Salamatin and others, 2003). To estimate the average growth rate of the air-hydrate crystals in the ice sheet, we assume that the age of the air-hydrate crystals is equivalent to the age below the top of the transition zone (~500 m depth). Figure 4 shows that the general trend of r with age in the 200–720 ka old ice is almost linear. This figure shows that the growth of the air-hydrate crystals occurred in two steps: the fast growth ($\sim 1 \times 10^{-6}$ mm a^{-1}) stage in the transition zone and the slow growth ($\sim 5 \times 10^{-8}$ mm a^{-1}) stage below the transition zone. The latter growth rate is similar to that observed in the Vostok ice core (Uchida and others, 1994a).

The growth process of air-hydrate crystals observed in the present study is different from that in the transition zone, where air bubbles and air hydrates coexisted. For the change in the distribution of the air-hydrate crystals in deep ice sheets, we may consider two possible mechanisms:

1. several air-hydrate crystals join together into one large crystal (coalescence process),
2. the larger crystals grow while the smaller crystals shrink (Ostwald ripening process).

Here we consider both mechanisms with regard to the Dome Fuji ice core.

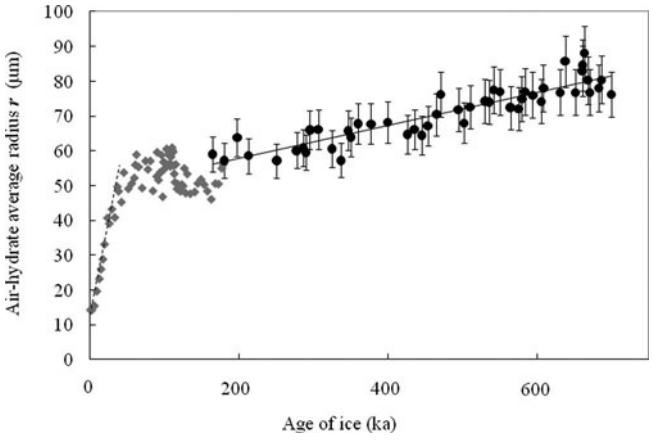

Fig. 4. Age profile of air-hydrate average radius r (solid circles: obtained in the present study; solid diamonds: obtained by Ohno and others, 2004). The ice-core age was estimated by comparison between the $\delta^{18}O$ data of Dome Fuji ice core (Motoyama and others, 2007) and the timescale of the EPICA Dome C (Antarctica) ice core (Parrenin and others, 2007).

https://doi.org/10.3189/002214311798843296 Published online by Cambridge University Press

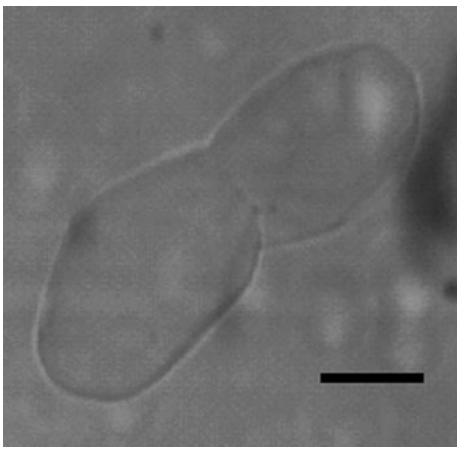

Fig. 5. Irregular type of air-hydrate crystal observed at 2962 m depth, considered to be formed by a two-crystal coalescence (with 100 μm scale bar).

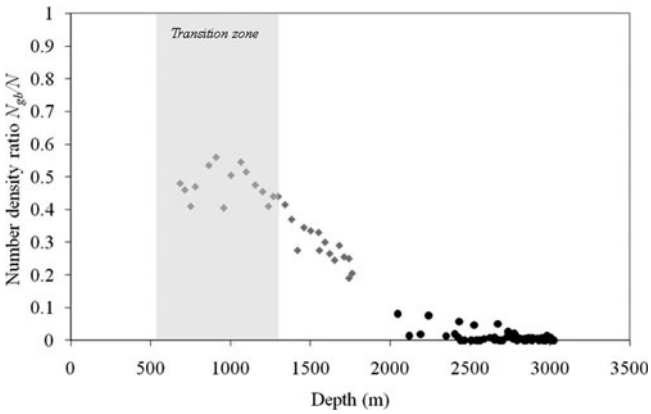

Fig. 6. Depth profile of number concentration ratio between air hydrates located on the ice grain boundary N_{gb} and N (solid circles: obtained in the present study; solid diamonds: obtained by Ohno and others, 2004). The hatched area indicates the transition zone.

The coalescence process may have occurred in the ice sheet because some of the air-hydrate crystals classified as irregular type seem to be a product of coalescence of two or more crystals (Figs 1c and 5). If the air-hydrate crystals join together, they may sinter to reduce the total interfacial area, i.e. to reduce the interfacial energy of the system. For this process to occur, the air-hydrate crystals must migrate through the ice matrix to join together because they are originally distributed widely, reflecting the air-bubble distribution. One of the major driving forces of air-hydrate migration is thought to be dragging due to grain boundary migration during ice grain growth. If this process was dominant, the air-hydrate crystals would be preferentially located on the ice grain boundary. Therefore, we examined the location of the air-hydrate crystals distributed in the ice matrix. Figure 6 shows the ratio of the number concentration of the air-hydrate crystals located on the ice grain boundary, N_{gb}, to the total number concentration, N. As stated previously (Ohno and others, 2004), N_{gb}/N decreased gradually with depth below the transition zone and reached an almost constant value that was very close to zero (below 2000 m, the average value of N_{gb}/N was ~1%). Figure 6 indicates that most of the air-hydrate crystals are located away from the ice grain boundaries below the transition zone. Detailed observations of the air-hydrate crystals (Uchida and others, 1993) revealed that air-hydrate crystals several hundred microns in size could not move easily with the grain boundary migrations. Therefore, we do not consider grain boundary migration to be very effective for air-hydrate migration, especially below the transition zone. As suggested by Kipfstuhl and others (2001), the existence of 'secondary clathrates' in the North Greenland Icecore Project (NorthGRIP) ice core would be one of the results of the coalescence process. These secondary clathrates are lengthy (>2 mm) rod-like crystals with smooth and regular, often polyhedral, shapes. If the air-hydrate crystals are very close together, coalescence may occur, possibly as a consequence of ice matrix deformation, in addition to the grain boundary migration. In Dome Fuji ice core, however, such closely distributed air-hydrate crystals do not appear to be common. Therefore, the coalescence process may have occurred mainly in the transition zone of the Dome Fuji ice core.

The second mechanism is air-hydrate crystal growth according to the Ostwald ripening process (Uchida and others, 1994b; Salamatin and others, 2003). The Ostwald ripening process is considered to be the major growth process of air-hydrate crystals below the transition zone because the source of air molecules for the crystal growth is the air-hydrate crystals themselves. When this process occurs, the large crystals grow gradually to compensate for the disappearance of the small crystals. Thus, the size distribution of the air-hydrate crystals changes with depth (see Figs 12–14 in Appendix B), a trend similar to that observed previously (Uchida and others, 1994a,b; Pauer and others, 1999; Lipenkov, 2000). Here we believe that the crystal growth rate is controlled mainly by air-molecule diffusion through the ice because the average growth rate of the air-hydrate crystals in the deep region is very small. If the kinetic process of crystal growth plays an important role, large amounts of faceted crystals should be observed. This process was mainly observed in the transition zone (Uchida and others, 1994c; Lipenkov, 2000; Ohno and others, 2004). However, the fact that most crystals below the transition zone are spherical suggests that the contribution of the kinetic process to the rate-determining process is small. Furthermore, the amount of heat transported during crystal growth is assumed to be negligible.

Diffusion is caused by the chemical potential difference between air molecules dissolved in the ice surrounding different-sized air-hydrate crystals, which depends on the total interfacial energy of the system. Because most of the air-hydrate crystals are located in the ice grains (see Fig. 6), we ignore the effect of grain boundaries, which are considered to be the highway of molecular diffusion. Here we employ a model similar to that proposed by Uchida and others (1994b), where large and small spherical crystals (with radii r_1 and r_2, respectively) are separated by a distance δ. The air concentrations in the ice matrix surrounding these crystals (q_1 and q_2, respectively) are different because of the Gibbs–Thomson effect. Thus, this air concentration gradient, $(q_2 - q_1)/\delta$, drives air molecules from the small crystals to the large ones, and the large crystals grow while the small ones shrink and finally disappear.

As we do not know the precise value for the gas solubility in ice, we estimate the permeation coefficient of the air molecules through the ice matrix $\langle \mathbf{D} \rangle$ to evaluate the diffusion of air in ice. Based on the crystal growth model (Uchida and others, 1994b), $\langle \mathbf{D} \rangle$ can be predicted by the

https://doi.org/10.3189/002214311798843296 Published online by Cambridge University Press

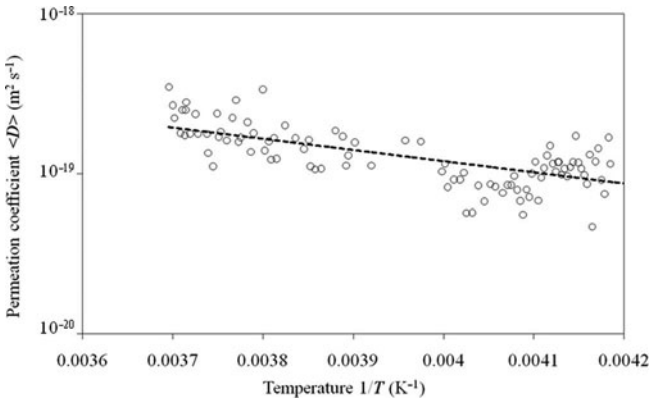

Fig. 7. Temperature dependence of permeation coefficient $\langle \mathbf{D} \rangle$ estimated using Equation (1). The dashed line indicates the linear regression implied by Equation (4).

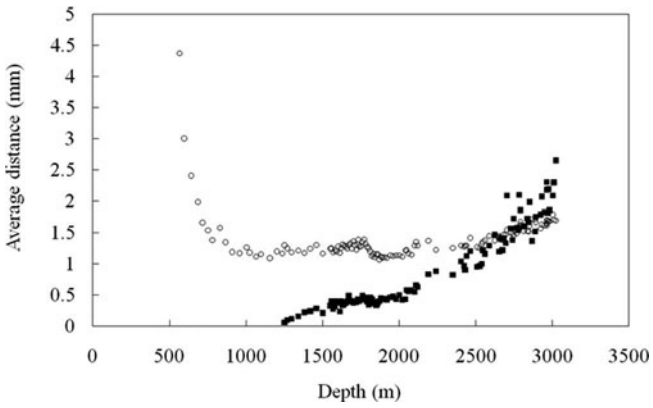

Fig. 8. Comparison of average inter-particle distance $N^{-1/3}$ (open circles) and distance of air-molecule migration below the transition zone $x(y)$ (solid squares).

product of the gas diffusion coefficient in ice, D_g, and the gas solubility in ice, C_{ge}, using the equation

$$\langle \mathbf{D} \rangle = D_g C_{ge} = \frac{dr_2}{dt} \frac{(\delta - r_2) r_2}{\delta} \frac{\Omega_i}{\Omega_{ah}} \left[\exp\left(\frac{2\Omega_{ah}\gamma_h}{kTr_1} \right) - \exp\left(\frac{2\Omega_{ah}\gamma_h}{kTr_2} \right) \right]^{-1}, \quad (1)$$

where Ω_i and Ω_{ah} denote the free volume of an air molecule in ice (3.35×10^{-20} mm^3) and in an air-hydrate crystal (2.4×10^{-19} mm^3), respectively. γ_h (6.3×10^{-8} J mm^{-2}) is the surface tension of the air-hydrate crystals (Uchida and others, 1993, along with the value of grain boundary energy shown in Hobbs, 1974), k is Boltzmann's constant and T is the in situ ice temperature. Two typical sizes of air-hydrate crystals, r_1 and r_2, are chosen from the size distribution function:

$$f_{LN}(r_1) = f_{LN}(r_2) = 0.5 f_{LN}(r)^{max} \quad (2a)$$

$$r_2 > r_1, \quad (2b)$$

where $f_{LN}(r)^{max}$ is the largest value of the fitted log-normal function. The average distance between the air-hydrate crystals is estimated as

$$\delta = N^{-1/3}. \quad (3)$$

It should be noted that the estimation of $\langle \mathbf{D} \rangle$ implies the permeation of an 'air' molecule, which is actually an average molecule of air through an ice matrix that excludes grain boundaries but includes impurities, lattice defects, etc. We then estimate $\langle \mathbf{D} \rangle$ at each depth using Equation (1). When we plot $\langle \mathbf{D} \rangle$ according to the Arrhenius equation (Fig. 7), we find the temperature dependence of $\langle \mathbf{D} \rangle$ below the transition zone,

$$\langle \mathbf{D} \rangle = \langle \mathbf{D} \rangle_0 \exp\left(-\frac{\langle \mathbf{Q} \rangle}{kT} \right), \quad (4)$$

and we can derive the constants $\langle \mathbf{D} \rangle_0 = (8 \pm 0.1) \times 10^{-17}$ m^2 s^{-1} and $\langle \mathbf{Q} \rangle = 13.4 \pm 1.4$ kJ mol^{-1}. Figure 7 indicates that the average permeation coefficient of the air molecules is very stable within the depth range below the transition zone, of the order of 10^{-19} m^2 s^{-1}, even though the ice temperature difference is ~40 K within this depth range.

Ikeda-Fukazawa and Hondoh (2003) summarized the previous model estimate of the permeation coefficients of N_2 and O_2 molecules in ice. They showed that $\langle \mathbf{D} \rangle$ was of the order of 10^{-19} m^2 s^{-1} at 263 K (Ikeda and others, 2000a) and 10^{-21} m^2 s^{-1} at 220 K (Salamatin and others, 2003); both estimates assumed $\langle \mathbf{Q} \rangle$ to be 50 kJ mol^{-1}. Although the range of $\langle \mathbf{D} \rangle$ in deep parts of the ice sheet seems to be similar to our estimation, $\langle \mathbf{Q} \rangle$ is very large. Later, simulation studies (Ikeda-Fukazawa and others, 2004a,b) suggested that the diffusion coefficients of both molecules used to estimate the permeation coefficients were 10^2 times larger than the previous value owing to another diffusion mechanism. Neither model prediction can explain our estimation. One possible reason is that the model predictions are based on a purified system such as in the case of a single crystal, whereas the present estimate is derived from the average value in a naturally complex system that includes grain boundaries, impurities, lattice defects, etc. Therefore, we conclude that our estimate of the permeation coefficient of air molecules in ice is the first direct evidence of air-molecule migration in ice sheets. It is possible to carry out a quantitative evaluation of the diffusion coefficient of air molecules in an ice matrix provided that we estimate the precise values of C_{ge} or the effect of various parameters that exist in the natural complex system mentioned above on D_g.

Using the $\langle \mathbf{D} \rangle$ data, we estimate the distance of air-molecule migration from an air-hydrate crystal driven by the Ostwald ripening process below the transition zone. The migration distance at each y, $x(y)$, is roughly estimated to be $(\langle \mathbf{D} \rangle \Delta t)^{-0.5}$, where Δt is the time period between the age of the ice at depth y and that at the bottom of the transition zone. If $x(y)$ reaches the value of δ at the same depth, the climatic information recorded in the air-hydrate distributions (observed in N and r) would clearly be modified due to the effective air molecule exchange. According to our estimate, $x(y)$ and δ become equal at depths below 2500 m (Fig. 8). This depth coincides with the depth where the disappearance of the climate-related variation of air-hydrate distributions becomes obvious. This is also consistent with the results shown in Figure 3.

Salamatin and others (2003) proposed a modified model to predict the effect of the growth of air-hydrate crystals in ice on the depth profiles of N and r in the deep ice core. Based on their model, climatically induced fluctuations in these profiles become damped with depth as the coarsening of smaller hydrates (in ice of the cold climate period) proceeds faster than the larger hydrates in ice of the warm climate period. They demonstrated that the values of the geometric parameters of air hydrates formed during cold

https://doi.org/10.3189/002214311798843296 Published online by Cambridge University Press

climate periods approach those in the interglacial ice in both the Vostok ice core and the GRIP ice core. The experimental results obtained in the present study strongly support their model prediction because the time period of crystal growth in the Dome Fuji ice core is much longer than in the other ice cores. This qualitative correlation between the actual profile and the model prediction also supports the claim that the crystal growth of air hydrates based on the Ostwald ripening effect plays an important role in the diminishing of the climatic records in deep ice sheets.

Recently, analysis of the O_2/N_2 ratio in ice cores has provided a chronology of the climatic changes over the past 360 ka (Kawamura and others, 2007). This ratio is considered to be a proxy for local summer insolation (Bender, 2002), which is recorded at the bubble close-off and preserved in air bubbles at shallower depths and in air-hydrate crystals at greater depths. However, Ikeda and others (1999) and Ikeda-Fukazawa and others (2001) found significant fractionation of air compositions between air bubbles and air-hydrate crystals in the transition zone. This fractionation is caused by the phase transition from air bubble to air-hydrate crystal because of the difference of the equilibrium partition between the N_2 and O_2 gas hydrates (Ikeda and others, 2000b). The fluctuation of the O_2/N_2 ratio must then be corrected below the transition zone (supplementary information of Kawamura and others, 2007). Based on the distribution of air-hydrate crystals in the Dome Fuji ice core, we can consider the long-term preservation of the O_2/N_2 ratio signal. As observed in Figure 8, the average distance of air-molecule diffusion in the ice matrix is ~1 mm over 345 ka. This is quantitatively too small a movement to affect the O_2/N_2 ratio record because the value of the O_2/N_2 ratio is the average of the sample thickness (usually several centimeters; Kawamura and others, 2003) along the depth axis. Thus, we consider that the air-hydrate crystal acts as a reliable container of ancient air molecules, which preserves the O_2/N_2 ratio over several hundred millennia. However, the spatial resolution of the O_2/N_2 ratio measurements will be limited by the air-molecule migration due to the air-hydrate crystal growth.

4. CONCLUSION

Microscopic observations of the air-hydrate crystals in the Dome Fuji ice core, Antarctica, below 2000 m, reveal the variations of the geometric parameters of air-hydrate distributions with depth. At depths below 2000 m, most of the air-hydrate crystals are spherical or ellipsoidal and are found inside the ice grains. The number concentration of the air-hydrate crystals decreases continuously with depth, whereas the average crystal size increases. These general trends are different from those observed at shallow depths (e.g. Ohno and others, 2004), suggesting that the variations in these parameters linked to palaeoclimatic changes may be reduced.

A detailed analysis of the observations of the air-hydrate crystals over the entire depth range of the Dome Fuji ice core reveals that the main reason for the distribution changes is the crystal growth of the air hydrates either by the coalescence process or by the Ostwald ripening process. Because the average radius of the air-hydrate crystals increases linearly with time (age of ice), the latter process is considered to be dominant at depths below the transition zone (~1250 m in the case of the Dome Fuji ice core). We also estimate the permeation coefficient of the air molecules in the ice from the geometric parameters of the air-hydrate distributions. The permeation coefficient at each depth is estimated to be of the order of $10^{-19}\,m^2\,s^{-1}$ between the bottom of the transition zone and the bottom of the borehole, although the ice temperature difference is ~40 K. The temperature dependence of the permeation coefficient is explained by the Arrhenius equation, and the activation energy for the air-molecule migration is found to be ~13.4 kJ mol^{-1}, which is very small compared to early model predictions (Ikeda-Fukazawa and others, 2001; Salamatin and others, 2003). The average migration distance of the air molecules estimated from the permeation coefficient is equivalent to the average distance between the air-hydrate crystals at depths below ~2500 m. Therefore, we believe that the smaller variation in the geometrical parameter of the air-hydrate distributions linked to the paleoclimatic changes is mainly caused by air-hydrate crystal growth accompanied by air-molecule migration through ice.

However, the impact of air-molecule migration in deep ice sheets on the paleoclimatic change records is estimated to be small, at least for the O_2/N_2 ratio record. If the depth resolution of gas analysis in the ice core increased to the order of millimeters, the effect of air-molecule migration would become a serious problem.

ACKNOWLEDGEMENTS

This study was partly supported financially by a grant for Creative Scientific Research (No. 14GS0202) from the Japanese Ministry of Education, Science, Sports and Culture. The authors thank the Dome Fuji drilling team for fieldwork, ice sampling and transportation, and logistic support. H. Ohno allowed us to reanalyze the distribution data of air-hydrate crystals in the shallow depths of the Dome Fuji ice core. We acknowledge S. Fujita for useful discussions regarding his unpublished grain-size data, K. Kawamura for detailed analysis of the O_2/N_2 ratio records and T. Ikeda-Fukazawa for simulation analysis. We also thank Y. Iizuka, T. Sakurai, K. Gohara and M. Nagayama for support during the distribution measurements held at the Institute of Low Temperature Science, Hokkaido University. We thank P. Duval, an anonymous reviewer and the scientific editor, D. Peel, for valuable comments and suggestions which improved the manuscript.

REFERENCES

Bender, M.L. 2002. Orbital tuning chronology for the Vostok climate record supported by trapped gas composition. *Earth Planet. Sci. Lett.,* **204**(1–2), 275–289.

Dome-F Deep Coring Group. 1998. Deep ice-core drilling at Dome Fuji and glaciological studies in east Dronning Maud Land, Antarctica. *Ann. Glaciol.,* **27**, 333–337.

EPICA Community Members. 2004. Eight glacial cycles from an Antarctic ice core. *Nature,* **429**(6992), 623–628.

EPICA Community Members. 2006. One-to-one coupling of glacial climate variability in Greenland and Antarctica. *Nature,* **444**(7116), 195–198.

Goto-Azuma, K. and Members of the Dome Fuji Ice Core Research Group. 2008. Millennial-scale climate variability during the past 720,000 years recorded in the Dome Fuji ice core. *Geophys. Res. Abstr.,* **10**, EGU2008-A-02971.

Hobbs, P.V. 1974. *Ice physics.* Oxford, etc., Clarendon Press.

Hondoh, T. 1989. Growth processes of clathrate-hydrate crystals in deep ice sheet. *J. Jpn Assoc. Cryst. Growth,* **16**(2), 149–161. [In Japanese with English summary.]

https://doi.org/10.3189/002214311798843296 Published online by Cambridge University Press

Hondoh, T., H. Anzai, A. Goto, S. Mae, A. Higashi and C.C. Langway, Jr. 1990. The crystallographic structure of the natural air-hydrate in Greenland Dye-3 deep ice core. *J. Incl. Phenom. Mol. Recogn. Chem.,* **8**(1–2), 17–24.

Ikeda, T., A.N. Salamatin, V.Ya. Lipenkov and T. Hondoh. 2000a. Diffusion of air molecules in polar ice sheets. *In* Hondoh, T., *ed. Physics of ice core records*. Sapporo, Hokkaido University Press, 393–421.

Ikeda, T., A.N. Salamatin, V.Ya. Lipenkov, S. Mae and T. Hondoh. 2000b. Spatial distribution of air molecules within individual clathrate hydrates in polar ice sheets. *Ann. Glaciol.,* **31**, 252–256.

Ikeda-Fukazawa, T. and T. Hondoh. 2003. Behavior of air molecules in polar ice sheets. *Mem. Natl Inst. Polar Res.,* Special issue 57, 178–186.

Ikeda-Fukazawa, T., T. Hondoh, T. Fukumura, H. Fukazawa and S. Mae. 2001. Variation in N_2/O_2 ratio of occluded air in Dome Fuji Antarctic ice. *J. Geophys. Res.,* **106**(D16), 17,799–17,810.

Ikeda-Fukazawa, T., K. Kawamura and T. Hondoh. 2004a. Diffusion of nitrogen gas in ice Ih. *Chem. Phys. Lett.,* **385**(5–6), 467–471.

Ikeda-Fukazawa, T., K. Kawamura and T. Hondoh. 2004b. Mechanism of molecular diffusion in ice crystals. *Mol. Simulat.,* **30**(13–15), 973–979.

Ikeda, T. *and 7 others*. 1999. Extreme fractionation of gases caused by formation of clathrate hydrates in Vostok Antarctic ice. *Geophys. Res. Lett.,* **26**(1), 91–94.

Johnsen, S.J., W. Dansgaard, H.B. Clausen and C.C. Langway, Jr. 1972. Oxygen isotope profiles through the Antarctic and Greenland ice sheets. *Nature,* **235**(5339), 429–434.

Kawamura, K., T. Nakazawa, S. Aoki, S. Sugawara, Y. Fujii and O. Watanabe. 2003. Atmospheric CO_2 variations over the last three glacial–interglacial climatic cycles deduced from the Dome Fuji deep ice core, Antarctica using a wet extraction technique. *Tellus B,* **55**(2), 126–137.

Kawamura, K. *and 17 others*. 2007. Northern Hemisphere forcing of climatic cycles in Antarctica over the past 360,000 years. *Nature,* **448**(7156), 912–916.

Kipfstuhl, S., F. Pauer, W.F. Kuhs and H. Shoji. 2001. Air bubbles and clathrate hydrates in the transition zone of the NGRIP deep ice core. *Geophys. Res. Lett.,* **28**(4), 591–594.

Lipenkov, V.Ya. 2000. Air bubbles and air-hydrate crystals in the Vostok ice core. *In* Hondoh, T., *ed. Physics of ice core records*. Sapporo, Hokkaido University Press, 327–358.

Lipenkov, V.Ya. and A.N. Salamatin. 1989. Relaksatsionnoye rasshireniye ledyanogo kerna iz burovoy skvazhini na st. Vostok [Volume relaxation of the ice core from the bore hole at Vostok station]. *Antarktika,* **28**, 59–72. [In Russian with English summary.]

Lipenkov, V.Ya., N.I. Barkov, P. Duval and P. Pimienta. 1989. Crystalline texture of the 2083 m ice core at Vostok Station, Antarctica. *J. Glaciol.,* **35**(121), 392–398.

Lüthi, D. *and 10 others*. 2010. CO_2 and O_2/N_2 variations in and just below the bubble-clathrate transformation zone of Antarctic ice cores. *Earth Planet. Sci. Lett.,* **297**(1–2), 226–233.

Miller, S.L. 1969. Clathrate hydrates of air in Antarctic ice. *Science,* **165**(3892), 489–490.

Miyamoto, A., T. Saito and T. Hondoh. 2009. Visual observation of volume relaxation under different storage temperatures in the Dome Fuji ice core, Antarctica. *In* Hondoh, T., *ed. Physics of ice core records II*. Sapporo, Hokkaido University Press, 73–79. (Supplement Issue of Low Temperature Science 68.)

Motoyama, H. 2007. The second deep ice coring project at Dome Fuji, Antarctica. *Sci. Drilling* 5, 41–43.

Motoyama, H. and Dome Fuji Ice Core Project Members. 2007. A new 3035.22m deep ice core at Dome Fuji, Antarctica and reconstruction of global climate and environmental change over past 720kyr. [Abstr. C51A-0076.] *Eos,* **88**(52), Fall Meet. Suppl.

Ohno, H., V.Ya. Lipenkov and T. Hondoh. 2004. Air bubble to clathrate hydrate transformation in polar ice sheets: a reconsideration based on the new data from Dome Fuji ice core. *Geophys. Res. Lett.,* **31**(L21), L21401. (10.1029/2004GL021151.)

Ohno, H., V.Ya. Lipenkov and T. Hondoh. 2010. Formation of air clathrate hydrates in polar ice sheets: heterogeneous nucleation induced by micro-inclusions. *J. Glaciol.,* **56**(199), 917–921.

Parrenin, F. *and 26 others*. 2007. The EDC3 chronology for the EPICA Dome C ice core. *Climate Past,* **3**(3), 485–497.

Pauer, F., S. Kipfstuhl, W.F. Kuhs and H. Shoji. 1999. Air clathrate crystals from the GRIP deep ice core: a number-, size- and shape-distribution study. *J. Glaciol.,* **45**(149), 22–30.

Petit, J.R. *and 18 others*. 1999. Climate and atmospheric history of the past 420,000 years from the Vostok ice core, Antarctica. *Nature,* **399**(6735), 429–436.

Salamatin, A.N., T. Hondoh, T. Uchida and V.Ya. Lipenkov. 1998. Post-nucleation conversion of an air bubble to clathrate air-hydrate crystal in ice. *J. Cryst. Growth,* **193**(1–2), 197–218.

Salamatin, A.N., V.Ya. Lipenkov and T. Hondoh. 2003. Air-hydrate crystal growth in polar ice. *J. Cryst. Growth,* **257**(3–4), 412–426.

Shoji, H. and C.C. Langway, Jr. 1982. Air hydrate inclusions in fresh ice core. *Nature,* **298**(5874), 548–550.

Sloan, E.D., Jr and C.A. Koh. 2008. *Clathrate hydrates of natural gases. Third edition.* Boca Raton, FL, CRC Press.

Uchida, T., S. Mae, T. Hondoh, P. Duval and V.Ya. Lipenkov. 1993. Measurements of surface energy of air-hydrate crystals in Vostok ice core, Antarctica. *Proc. NIPR Symp. Polar Meteorol. Glaciol.,* **7**, 1–6.

Uchida, T., T. Hondoh, S. Mae, V.Ya. Lipenkov and P. Duval. 1994a. Air-hydrate crystals in deep ice-core samples from Vostok Station, Antarctica. *J. Glaciol.,* **40**(134), 79–86.

Uchida, T., S. Mae, T. Hondoh, V.Ya. Lipenkov, P. Duval and J. Kawabata. 1994b. Growth process of air-hydrates and diffusion of air molecules in deep ice sheet. *Proc. NIPR Symp. Polar Meteorol. Glaciol.,* **8**, 140–148.

Uchida, T., P. Duval, V.Ya. Lipenkov, T. Hondoh, S. Mae and H. Shoji. 1994c. Brittle zone and air-hydrate formation in polar ice sheets. *Mem. Natl Inst. Polar Res.,* Special Issue 49, 298–305.

Uchida, T., T. Hondoh, S. Mae, H. Shoji and N. Azuma. 1994d. Optimized storage condition of deep ice core samples from the viewpoint of air-hydrate analysis. *Mem. Natl Inst. Polar Res.,* Special Issue 49, 306–313.

Van der Waals, J.H. and J.C. Platteeuw. 1959. Clathrate solutions. *Adv. Chem. Phys.,* **2**(1), 1–57.

Watanabe, O., J. Jouzel, S. Johnsen, F. Parrenin, H. Shoji and N. Yoshida. 2003. Homogeneous climate variability across East Antarctica over the past three glacial cycles. *Nature,* **422**(6931), 509–512.

APPENDIX A. ESTIMATION OF EXPERIMENTAL UNCERTAINTIES

A.1. Uncertainty estimation of *N*

The microscale nonuniformity of the spatial distribution of air-hydrate crystals ($N \pm \delta N$) is obtained by frequent measurements in the same thin section. The following four thin sections were measured along three different optical lines:

a. Estimated N values on three measurement lines at 2653.5 m depth: 0.347 ± 0.020 [mm^{-3}]

b. Estimated N values on three measurement lines at 2775 m depth: 0.258 ± 0.012 [mm^{-3}]

c. Estimated N values on three measurement lines at 2793 m depth: 0.234 ± 0.018 [mm^{-3}]

d. Estimated N values on three measurement lines at 2962.5 m depth: 0.221 ± 0.019 [mm^{-3}]

Thus, we estimate the experimental uncertainties of the N estimation for each measurement as the maximum uncertainty of the above calibration measurements,

https://doi.org/10.3189/002214311798843296 Published online by Cambridge University Press

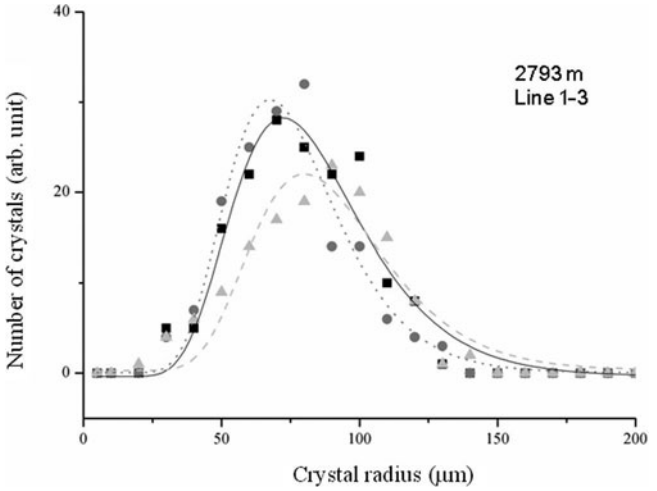

Fig. 9. Comparison of r distributions measured on three different optical lines in the same ice piece (2793 m). Each line indicates a log-normal fitting curve.

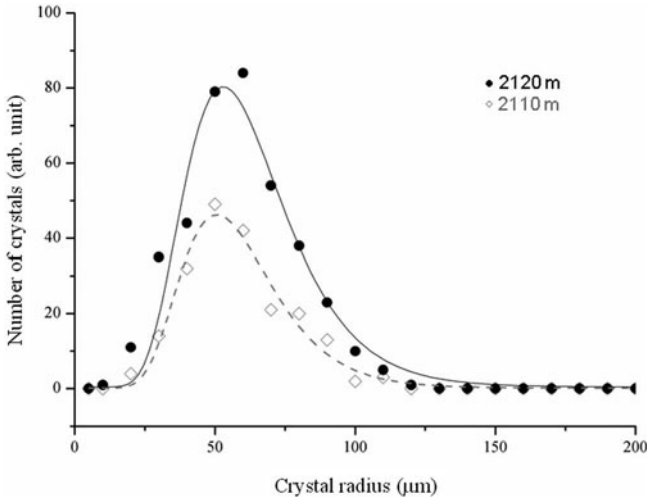

Fig. 10. Comparison of r distributions measured on different thin sections prepared from nearby depths and measured by different researchers (2120 m: solid circle, present study; 2110 m: open diamond, Ohno and others, 2004). Each line indicates the log-normal fitting curve.

$(\delta n/N)_{max} = 8.6\%$, which is shown on the data obtained in the present study in Figures 2a and 3a. This uncertainty is comparable to that found in the Vostok ice-core analysis (Uchida and others, 1994a; Lipenkov, 2000).

The consistency of measurements in the present study with those of previous measurements (Ohno and others, 2004) is tested by comparing the value of N measured at similar depths. Here we compare N values at $y = 2120$ m in the present study with those at 2110 m in a previous study (Ohno and others, 2004).

$$N(2120) = 0.461 \pm 0.040 \ [\mathrm{mm}^{-3}]$$

$$N(2110) = 0.408 \pm 0.035 \ [\mathrm{mm}^{-3}]$$

The agreement is considered reasonable, taking into consideration the measurement uncertainty of N and the difference in depth.

A.2. Uncertainty estimation of r

The microscale nonuniformity of the spatial distribution of air-hydrate crystals also results in an uncertainty in the estimation of r. In order to show the validity of r estimates in the present study, we estimate the difference of the distribution of r between repeated measurements in the same thin section. The following four thin sections were measured three times along different optical lines ($r \pm \delta r$) (Fig. 9).

a. Estimated r values on three measurement lines at 2653.5 m depth: 64.7 ± 2.4 [μm]

b. Estimated r values on three measurement lines at 2775 m depth: 74.0 ± 4.6 [μm]

c. Estimated r values on three measurement lines at 2793 m depth: 76.9 ± 6.6 [μm]

d. Estimated r values on three measurement lines at 2962.5 m depth: 82.9 ± 2.8 [μm]

Thus, we estimate the experimental uncertainties of r estimation for each measurement as the maximum uncertainty of the above calibration measurements, $(\delta r/r)_{max} = 8.6\%$, which is shown on the data obtained in the present study in Figures 2b and 3b. More than 200 crystals were measured for each thin section. The uncertainty is thus comparable to that of Vostok ice-core analysis (Uchida and others, 1994a; Lipenkov, 2000).

On the other hand, the consistency of measurements in the present study with previous measurements (Ohno and others, 2004) is tested by comparing the measured r distributions at similar depths. Here we compare the parameters of r distributions fitted by the log-normal distribution (mean radius $\langle r \rangle$ and standard deviation σ) at $y = 2120$ m in the present study with data from 2110 m in a previous study (Ohno and others, 2004) (Fig. 10).

$$\langle r \rangle \ (2120\ \mathrm{m}) = 57.2 \pm 4.9 \ [\mu\mathrm{m}], \ \sigma = 0.36$$

$$\langle r \rangle \ (2110\ \mathrm{m}) = 56.1 \pm 4.8 \ [\mu\mathrm{m}], \ \sigma = 0.32$$

The agreement is considered reasonable, taking into consideration the measurement uncertainty of r and the difference in depth. The standard deviation of the log-normal fitting for r is almost independent of depth (Fig. 11). Therefore, we may conclude that the measurements in the present study are consistent with previous measurements (Ohno and others, 2004).

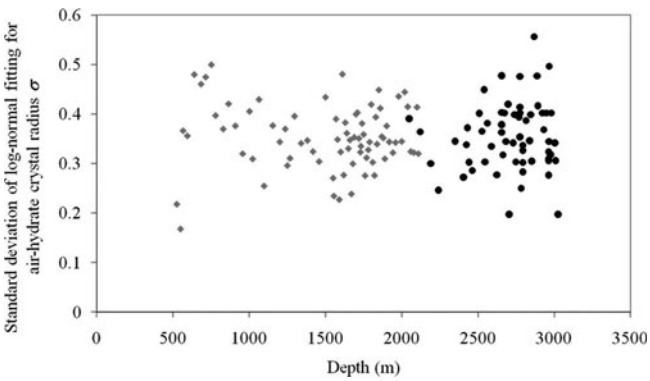

Fig. 11. Standard deviation of log-normal fitting for r (black solid circles: obtained in the present study; gray solid diamonds: obtained by Ohno and others, 2004).

https://doi.org/10.3189/002214311798843296 Published online by Cambridge University Press

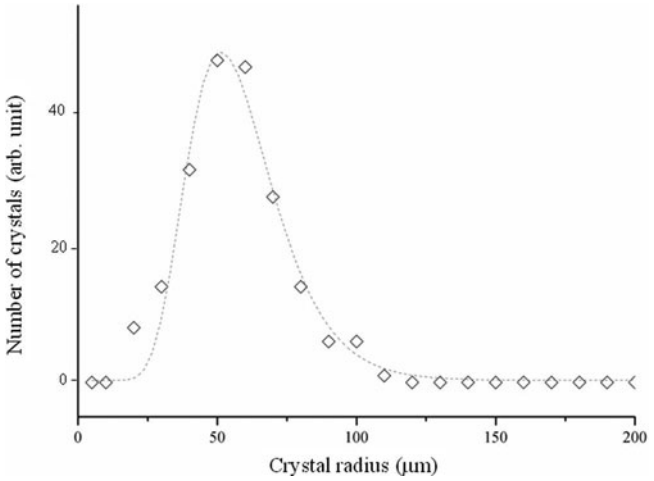

Fig. 12. Reanalyzed *r* distributions in 1250 m ice core. The line indicates the log-normal fitting curve.

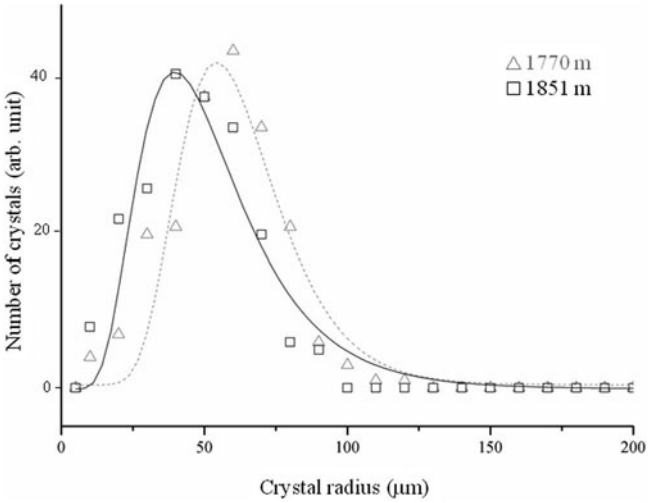

Fig. 13. Comparison of *r* distributions between glacial (1851 m: open squares) and interglacial (1770 m: open triangles) ice (reanalyzed from Ohno and others, 2004). Each line indicates the log-normal fitting curve.

APPENDIX B. CRYSTAL SIZE DISTRIBUTIONS OF AIR HYDRATES WITH DEPTH

Some of the radius distributions of air-hydrate crystals are shown here.

1. The *r* distributions at the bottom of the transition zone (1250 m), reanalyzed from previous measurements (Ohno and others, 2004) are shown in Figure 12.
2. Comparison of the size distributions between glacial ice and interglacial ice:

(a) Termination II (glacial ice: open squares; interglacial ice: open triangles), which is reanalyzed from previous measurements (Ohno and others, 2004) (Fig. 13)

(b) Termination IV (glacial ice: black solid squares; interglacial ice: gray solid triangles) obtained in the present study (Fig. 14).

When we compare the radius distributions between glacial and interglacial ice around terminations II and IV, we notice an obvious shift in the peak value of *r* between the glacial and interglacial ice at termination II, although other parameters of the log-normal fitting curves are almost the same. At termination IV, on the other hand, the radius distributions of air-hydrate crystals between glacial and interglacial ice do not shift significantly. Uchida and others (1994a) and Salamatin and others (2003) predicted that this distribution change could be caused by the preferential growth of larger crystals. More precise measurements and a comparison with model calculations will reveal the process that causes the diminishing of the climate change information from air-hydrate distributions.

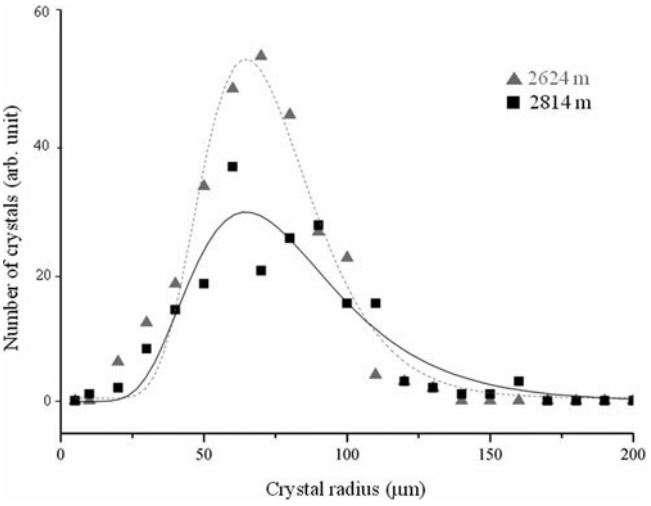

Fig. 14. Comparison of *r* distributions between glacial (2814 m: black solid square) and interglacial (2624 m: gray solid triangle) ice. Each line indicates the log-normal fitting curve.

MS received 18 February 2011 and accepted in revised form 19 August 2011

https://doi.org/10.3189/002214311798843296 Published online by Cambridge University Press